Developmental Biology 322 (2008) 109–120

Contents lists available at ScienceDirect

Developmental Biology

journal homepage: www.elsevier.com/developmentalbiology

Spatial and temporal segregation of auditory and vestibular neurons in the otic placode

Donald Bell [a], Andrea Streit [a], Itziar Gorospe [b], Isabel Varela-Nieto [b], Berta Alsina [c], Fernando Giraldez [c,*]

[a] Department of Craniofacial Development, King's College London, London SE1 9RT, UK
[b] Instituto de Investigaciones Biomédicas "Alberto Sols", (CSIC-UAM) CIBER-ER, c/Arturo Duperier 4, 28029 Madrid, Spain
[c] CEXS, Universitat Pompeu Fabra, Parc de Recerca Biomèdica de Barcelona (UPF-PRBB), Dr. Aiguader 88, 08001, Barcelona, Spain

ARTICLE INFO

Article history:
Received for publication 6 June 2008
Revised 9 July 2008
Accepted 9 July 2008
Available online 19 July 2008

Keywords:
Chick
Cochlear–vestibular ganglion
Ear development
Neuroblast
Neurogenesis
Otic vesicle
Proneural genes
Sensory precursors
Temporal specification

ABSTRACT

The otic placode generates the auditory and vestibular sense organs and their afferent neurons; however, how auditory and vestibular fates are specified is unknown. We have generated a fate map of the otic placode and show that precursors for vestibular and auditory cells are regionally segregated in the otic epithelium. The anterior-lateral portion of the otic placode generates vestibular neurons, whereas the posterior-medial region gives rise to auditory neurons. Precursors for vestibular and auditory sense organs show the same distribution. Thus, different regions of the otic placode correspond to particular sense organs and their innervating neurons. Neurons from contiguous domains rarely intermingle suggesting that the regional organisation of the otic placode dictates positional cues to otic neurons. But, in addition, vestibular and cochlear neurogenesis also follows a stereotyped temporal pattern. Precursors from the anterior-lateral otic placode delaminate earlier than those from its medial-posterior portion. The expression of the proneural genes *NeuroM* and *NeuroD* reflects the sequence of neuroblast formation and differentiation. Both genes are transiently expressed in vestibular and then in cochlear neuroblasts, while differentiated neurons express Islet1, Tuj1 and *TrkC*, but not *NeuroM* or *NeuroD*. Together, our results indicate that the position of precursors within the otic placode confers identity to sensory organs and to the corresponding otic neurons. In addition, positional information is integrated with temporal cues that coordinate neurogenesis and sensory differentiation.

Introduction

The vertebrate adult inner ear is a complex sensory organ responsible for hearing and balance. The dorsal domain of the inner ear, the vestibular system, specialises in detection of angular and linear acceleration and the ventral domain, the auditory (cochlear) organ is sensitive to sound. Hair cells transduce deflections of bundles of stereocilia into electrical signals, which in turn activate bipolar sensory neurons that reside in the vestibular and the auditory/cochlear ganglion (VG and CG, respectively). Thereby, sensory stimuli are transmitted from the hair cells located in the sensory organs to the specialised sensory nuclei in the brainstem (for review see: Rubel and Fritzsch, 2002; Alsina et al., 2003).

Otic neurons derive from the otic placode (D'Amico-Martel and Noden, 1983). Their generation is a sequential process, which includes the specification of neuronal precursors in the otic epithelium, delamination of neuroblasts, proliferation of neuroblasts in the cochlear–vestibular ganglion (CVG) and, finally, differentiation of neurons that project to the sensory epithelia and to the brain (for review see Rubel and Fritzsch, 2002; Alsina et al., 2003). The region of the otic placode that contains neuronal precursors has recently been mapped to the anterior-medial region of the otic placode, the proneural domain (Alsina et al., 2004; Abelló et al., 2007). Neuroblasts condense to form the CVG, which develops further into separate cochlear and vestibular parts that are present in the adult. Otic neurons seem to have stereotyped guidance behaviours, indicating that the bias to innervate specific targets of the ear occurs early during the process of neurogenesis (Koundakjian et al., 2007; for review see: Rubel and Fritzsch, 2002; Fekete and Campero, 2007). However, little is known about the mechanisms that specify auditory and vestibular neurons.

A different but related problem is whether the neurons in the otic epithelium originate from same locations as the sensory structures they will later innervate (Fekete and Campero, 2007). In mice it has been suggested that cochlear neurons arise from the primordia of the cochlear epithelium and then project back to the same region of the cochlea (Altman and Bayer, 1982; Carney and Silver, 1983), but the opposite conclusion has been reached in the chick (Noden and van deWater, 1986; see Rubel and Fritzsch, 2002). These studies were based on morphological observations and only few data are available using direct cell tracing. Current evidence suggests that neurons and sensory cells share a common progenitor (Satoh and Fekete, 2005). In mouse a common

* Corresponding author.
E-mail address: fernando.giraldez@upf.edu (F. Giraldez).

0012-1606/$ – see front matter © 2008 Elsevier Inc. All rights reserved.
doi:10.1016/j.ydbio.2008.07.011

Neurogenin1 (*Neurog1*) expressing region contributes to the CVG as well as to macular and non-sensory epithelia associated with the maculae and cristae (Raft et al., 2007), but the lineage relationship between sensory cristae and the corresponding neurons remains unclear. The expression profiles of *BMP4* and *Lfng* in the mouse otocyst may suggest that neurons innervating the cristae may not arise from the regions destined to form cristae (Morsli et al., 1998).

Within the otic placode, the neurogenic domain is defined by the expression of proneural genes, which are basic helix–loop–helix (bHLH) genes with homology to *Drosophila melanogaster* proneural gene *atonal* (*Atoh*) that control cell fate decisions, such as neurogenesis and myogenesis in vertebrates and invertebrates (Campuzano and Modolell, 1992; Bertrand et al., 2002). The development of otic neurons depends on the expression of specific proneural genes, and the inactivation of *Neurog1* or *NeuroD (NeuroD1)* in the mouse ear causes a reduction in the number of neurons (Liu et al., 2000; Ma et al., 2000; Kim et al., 2001; for review see Sanchez-Calderon et al., 2007). In vertebrates, proneural genes have been shown to specify not only generic neuronal fate, but also specific neuronal subtypes, although this possibility has not been explored in the ear (Bertrand et al., 2002; Parras et al., 2002; Lee and Pfaff, 2003).

The present work investigates the origin of auditory and vestibular neuron subtypes in the otic placode by fate and gene mapping. We show that the precursors of the vestibular and auditory neurons are physically segregated in the otic placode, and that vestibular neurons are generated prior to auditory neurons. Interestingly, the origin of sensory organs overlaps with the corresponding innervating neurons. *NeuroD* and *NeuroM* (*NeuroD4*) are expressed transiently in the otic epithelium, first in vestibular and then in auditory neurons, indicating that they label the sequence of neuron production rather than neuronal subtype. These results suggest that the specification of vestibular and auditory identity relies on both temporal and positional information in the otic placode.

Materials and methods

Embryo techniques and sections

Fertile hens' eggs were purchased from Winter Farm (UK) and Granja Gibert, Tarragona (Spain) and incubated at 38 °C in a humidified incubator until the desired stage (Hamburger and Hamilton, 1951). For fate mapping experiments, eggs were windowed and injected with Indian ink (Pelikan, 1:20 in Tyrode's saline). Using a tungsten needle the vitelline membrane was opened and small cell populations in the otic cup/vesicle were labelled with DiI (0.5% in absolute alcohol, diluted 1:10 in 0.3 M sucrose) and DiO (0.25% in absolute alcohol, diluted 1:10 in 0.3 M sucrose) using microcapillaries and air pressure (Stern, 1998). The position of each injection was recorded or in some cases photographed using epifluorescence. Eggs were sealed using insulating tape and further incubated until E7.

Embryos were fixed overnight in 4% formaldehyde in phosphate buffered saline (PBS), washed in PBS before being placed in 1 ml acrylamide working solution (10% acrylamide:bisacrylamide stock [37.5:1 acrylamide:bisacrylamide], 0.33% TEMED, in PBS) at 50 °C for 30 min. They were then embedded by adding 3 ml 4% agarose in PBS and 100 µl ammonium persulfate (20 mg/ml) and allowed to set at room temperature (adapted from Germroth et al., 1995) Embryos were sectioned sagittally at 200 µm using a vibratome (Leica); sections were stored in the dark in PBS containing 0.02% sodium azide until examination.

Chi squared analysis was carried out, using Microsoft Excel, on tabulated data with 'expected' values being calculated under the null hypothesis that there is no spatial bias to where a particular label will end up.

In situ hybridisation

Whole-mount *in situ* hybridisation was performed as described (Henrique et al., 1995) using digoxigenin (DIG) labelled RNA probes for chick *NeuroD*, *NeuroM* and *Trkc* (EST65J22). After hybridisation embryos were washed with solution I (50% formamide, 1% SDS, 5× SSC pH 4,5), solution II (50% formamide, 2× SSC) and TBST (150 mM NaCl, 10 mM KCl, 25 mM Tris pH 7.5, 0.1% Tween-20). Then, embryos were blocked at room temperature with 10% goat serum in TBST and incubated overnight with anti-digoxigenin antibody coupled to alkaline phosphatase (Roche, 1/2000) and detected with NBT/BCIP in NTMT (100 mM NaCl, 100 mM Tris–HCl pH 9,5, 50 mM $MgCl_2$, 0.1% Tween-20).

In situ hybridisation on sections was carried out using the same probes as above; hybridisation was carried out over night at 65 °C. Sections were rinsed with 50% formamide and 1× SSC followed by TBST and blocked at room temperature with 2% Blocking Reagent (Roche), 10% goat serum in TBST and incubated overnight with anti DIG antibody (1/2000) and detected with NBT/BCIP in NTMT. Fluorescent detection of transcripts was performed in some cases like in Figs. 7B and C, using Fast Red (Sigma F4523).

Immunohistochemistry

Immunohistochemistry after *in situ* hybridisation was used to detect Islet1 and Tuj1. Sections were blocked at room temperature with 2% bovine serum albumin (BSA, Sigma) and 5% goat serum in PBT (PBS and 0.1% Tween) for 90 min, incubated overnight with the primary antibody (in 2% BSA, 5% goat serum), washed with the same solution, and incubated with secondary antibodies overnight. Sections were rinsed several times in PBT before mounting in Vectashield. Anti-Islet1/2 monoclonal antibody (39.4D5, DSHB, 1:200) and anti-Tuj1 polyclonal antibody (PRB-435P, Covance, 1:200) were used as primary antibodies, while goat anti-rabbit Alexa 594, anti-rabbit Alexa 488 and goat anti-mouse Alexa 488 (Molecular Probes; 1:400) were used as secondary antibodies.

Results

To understand how and when specific cell identities within the otic placode are acquired we produced a fate map of the proneural domain before and during neuroblast delamination. Small cell populations in the placode and cup were labelled with the lipophilic dyes DiI and DiO between HH10 and HH17 (E1.5–E3.5), during which most of the delamination process occurs. Embryos were allowed to develop until HH30–32 (E7) and the position of labelled cells was scored in the otic epithelium and the CVG. At this stage the inner ear and CVG have developed the elements present in the adult and the different branches of the CVG projecting to discrete sensory organs can be distinguished (Fig. 1A). Fate maps were produced by plotting scored labels, colour-coded according to their fate onto a diagram of a dorsal view of the otic placode or cup at the time of labelling (Figs. 1B, D). The proneural domain, as defined by gene expression patterns occupies the anterior-medial half of the otic cup (Alsina et al., 2004; Abelló et al., 2007, see also Figs. 6A–F), where the majority of labels were applied.

Origin of cochlear and vestibular neurons

The precise position of labelled neurons was determined according to their location within four anatomically distinct parts of the CVG (Fig. 1A). Dorsally, the anterior-lateral vestibular nerve (ALVN) innervates the lateral and anterior cristae (orange and yellow, respectively), while the posterior vestibular nerve (PVN) projects to the posterior crista (pink). The anterior and inferior domain of the vestibular ganglion innervates the maculae (IVG, purple) and most

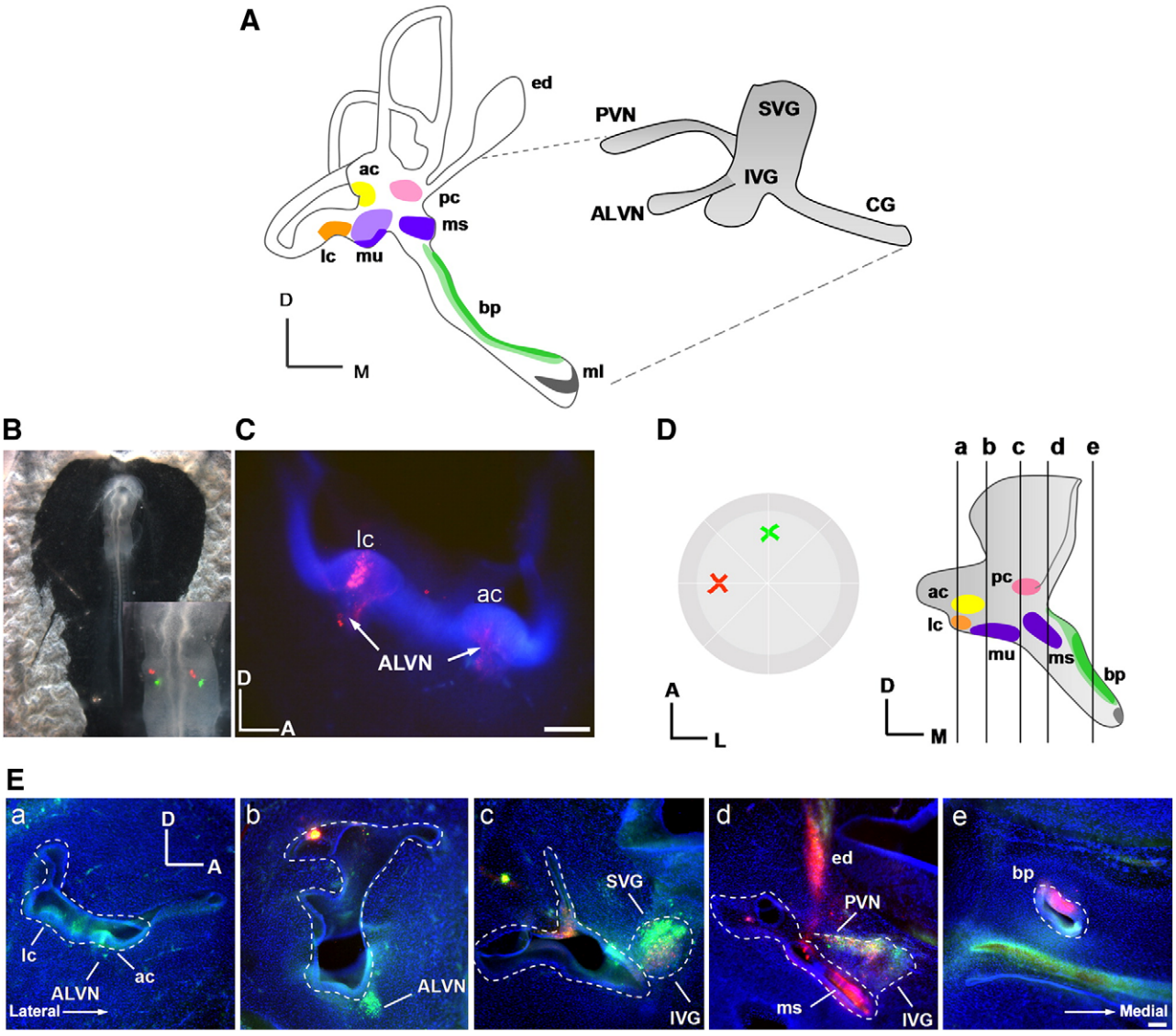

Fig. 1. Anatomical divisions of the ear and examples of DiI and DiO labelling. (A) Schematic drawing of the inner ear and its innervation at HH30–31 (E7). Anterior crista (ac): yellow, lateral crista (lc): orange, posterior crista (pc): pink, utricular and saccular maculae (mu and ms): purple, basilar papilla (bp): green. ed: endolymphatic duct. The anterior-lateral vestibular nerve (ALVN) innervates ac and lc, the inferior vestibular ganglion (IVG) projects to the maculae, the posterior vestibular nerve (PVN) to the pc and cochlear ganglion (CG) to the bp. (B) Dorsal view of HH11 embryo showing typical DiI and DiO labelling of both otic cups. Inset: close-up of the otic region. (C) DiI labelling similar to the left otic cup in panel A. Lateral sagittal section at HH30 shows DiI-labelled cells in sensory epithelium of the lc (but not ac) and in ALVN innervating both ac and lc. Size bar is 100 μm; dorsal to the top, anterior to the right. (D) Diagram illustrating the analysis of a typical experiment. On the left, the wheel shows the location of the injections. The dark grey rim represents the otic ridge that separates the otic domain from non-otic ectoderm. The diagram on the right shows the section planes for analysis at HH30–31. (E) The otic placode was labelled with DiI medially and DiO laterally at HH10 and analysed at HH30–31. Five panels (a–e) showing sagittal sections of a single DiI and DiO labelled inner ear as illustrated in panel D. DiO remains in the more dorsal and lateral structures and nerve branches, while DiI labels more medial and ventral domains, including the macula sacculi and the basilar papilla, with some intermingling in the PVN and the intermediate region of the VG. Abbreviations as in panel A.

ventrally the cochlear ganglion innervates the basilar papilla (CG, green). This corresponds to the dorsal/ventral (D/V) organisation of sensory organs, with the three cristae located most dorsally followed by the maculae and the cochlea ventrally. The anatomical separation of vestibular and cochlear neurons is clear, while vestibular branches that innervate utricular and saccular maculae are difficult to distinguish and were therefore pooled together for the analysis.

In total 189 embryos were labelled at HH10-12 and received DiI and DiO injections simultaneously in distinct regions of each otic placode (Fig. 1B). Labelling in at least part of the CVG was observed in 89% of specimens, but only in 67% it was possible to allocate labelled cells accurately to at least one of the four anatomical divisions and so only these were used to generate the fate maps. One example of labelled cristae and ALVN is shown in Fig. 1C. When the placode is labelled medially with DiI and laterally with DiO (Fig. 1B, right otic placode; diagram in Fig. 1D), DiO labelled cells are found in the anterior-lateral nerves and cristae, as well as in the superior part of the vestibular ganglion (Fig. 1Ea–c), and DiI-labelled cells are present in the IVG, the macula saccularis, the basilar papilla and the base of the endolymphatic duct (Fig. 1Ec–e) at stage HH31 (E7). Fluorescent cells in the ganglia always locate to discrete regions with little cell mixing (Fig. 1Ec).

The resulting maps reveal a spatial segregation of neuronal precursors within the otic cup (Fig. 2A). Its anterior and lateral domain preferably gives rise to the innervation of the anterior and lateral cristae (Fig. 2A yellow, see example in Figs. 1C and Ea–c), while its anterior and medial portion gives rise to macular neurons (Fig. 3A purple), and the posterior-medial otic placode contains the precursors of cochlear neurons (Fig. 3A green; see also Fig. 1Ec–d). Prospective neurons innervating the posterior crista (Fig. 2A pink) intermingle

with IVG and CG precursors. To analyse this segregation in more detail, we examined how often a single injection contributes to only one or more branches of the CVG: the ALVN, the IVG and the CG are usually labelled alone, whereas the PVN is equally likely to be co-labelled with one of the other branches of the vestibular nerve (Fig. 2B). This is also illustrated in the Venn diagram in Fig. 2C where coloured peripheral areas represent injections resulting in a single CVG domain, and overlapping areas represent those cases in which a single injection gives rise to more than one domain of the CVG. Only few samples (8/29, 28%) show co-labelling of the cochlear nerve and the vestibular ganglia, and conversely, the probability of co-labelling the vestibular ganglia and the auditory nerve is also very low (21/182, 12%, see Figs. 2B and C). Labelling of more than two nerve branches is rare except for the combination of ALVN, IVN and PVN. It is possible, however, that this reflects a slightly larger initial label than a true overlap of precursor populations. These findings suggest that already at the placode or early cup stage, neuronal precursors of different fates are located in defined positions. The anterior-lateral part contains mainly neuronal precursors that project to the anterior and lateral cristae, the anterior-medial portion forms neurons projecting to the posterior crista and maculae, whilst the most posterior and medial portion of the proneural domain largely generates neurons that innervate hair cells in the cochlear duct and posterior cristae. Thus, the D/V axis of the ganglion is represented along the anterior-lateral/posterior-medial axis in the otic placode.

Sequential neuroblast delamination from different regions of the otic cup

Recent data in the mouse suggest an early temporal segregation of cochlear and vestibular precursors (Koundakjian et al., 2007). To investigate whether this may also be the case in chick, we carried out experiments in which embryos were either collected at different times after labelling, or injected with two different dyes in a sequential manner. When the otic placode (HH11) is labelled with DiO anterior-laterally and with DiI medially, after 24 h DiO-labelled cells (Fig. 3Aa–f; green) have delaminated into the forming CVG, whereas cells from the medial otic cup remain in the epithelium (Fig. 3Aa–f; red; $n=8$). Forty-eight hours after dye injection, descendants from the anterior-lateral placode (green) are found predominantly in the most dorsal part of the CVG, while the progeny of the medial placode (red) is still visible in the epithelium and has started to populate the most ventral and proximal parts of the CVG (Fig. 3Ag, h; $n=7$). There is little mixing between both cell populations (Fig. 3Ah). Thus, neuroblasts from the medial otic placode delaminate later than the precursors that innervate dorsal structures (cristae).

In another set of experiments the otic cup was first labelled with DiI at HH12–13 (E2), with DiO at HH17–18 (E3; Fig. 3B) and then allowed to develop for another 48 h. Those injections were deliberately large to ensure labelling of the whole proneural domain. In this experiments ($n=4$), early DiI-labelled cells (red) contribute to

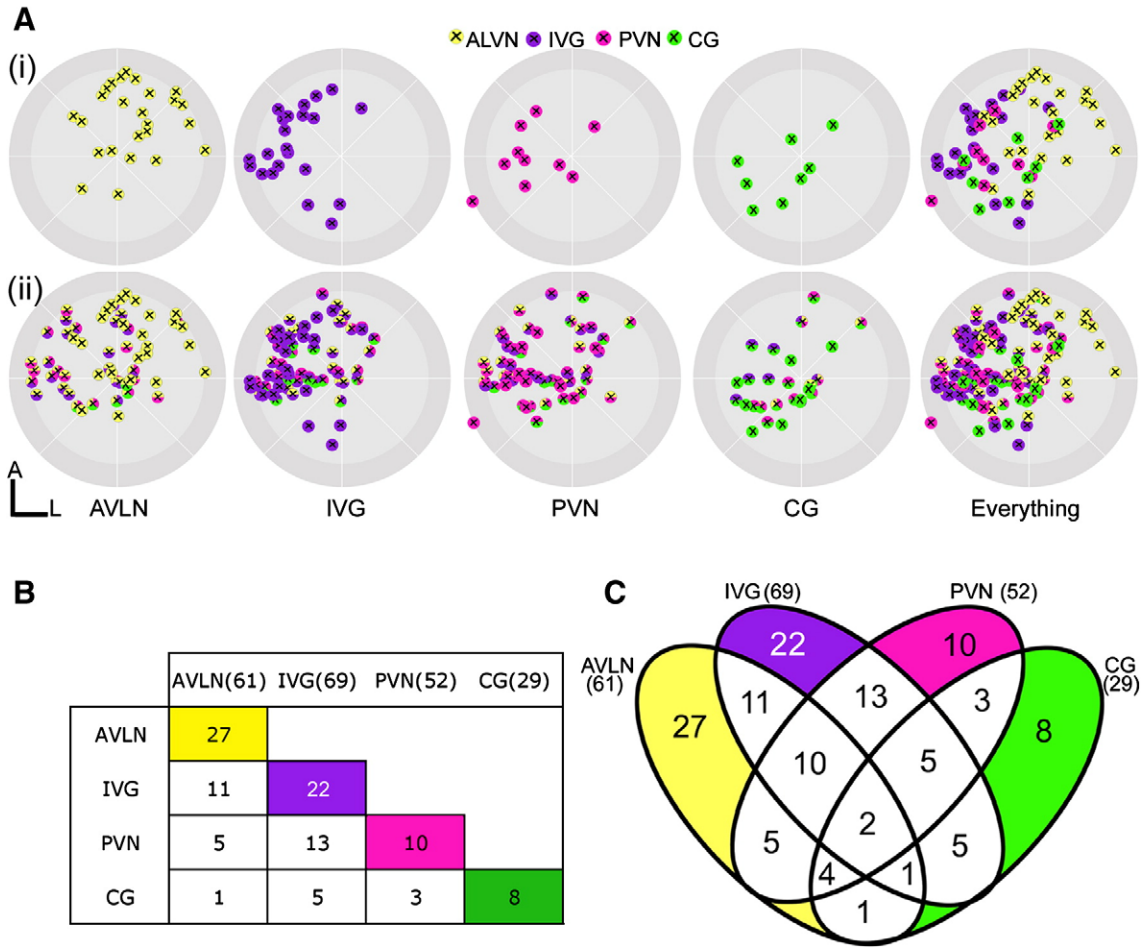

Fig. 2. The origin of neurons in the otic placode. (A) Maps showing the position of neuronal precursors in a schematised otic cup of HH10–11, anterior is to the top and lateral to the right. Fates of neurons (dots with crosses) are colour-coded: ALVN yellow, IVG purple, PVN pink and CG green. (i) The top panels show instances where only one of the nerve branches was labelled, equivalent to the coloured boxes/petals in panels B and C. (ii) Panels show the spatial arrangement of all the nerve labelling data from panel C including instances where more than one nerve branch was labelled (indicated by dots of more than one colour). (B) Frequency of injections giving rise to simple combinations of nerve labelling. (C) Venn diagram showing the frequency of all possible nerve labelling combinations.

both the vestibular and cochlear ganglion, however, DiO labelled progeny (green) is only observed in the most ventral VG and in the CG. Note that the ALVN and PVN, which innervate cristae, and the superior vestibular ganglion, are labelled only by DiI (Fig. 3Ba–c). More ventral sections show double-labelled cells in yellow (yellow arrows). Therefore, early injections label all neuronal subtypes, while late injections only label the ventral portion of the vestibular ganglion and the cochlear ganglion, suggesting that precursors of the dorsal CVG delaminate before those of the ventral CVG. Together, these results suggest that a temporal sequence of neuroblast delamination and neuron production is superimposed onto the spatial segregation of in the otic placode.

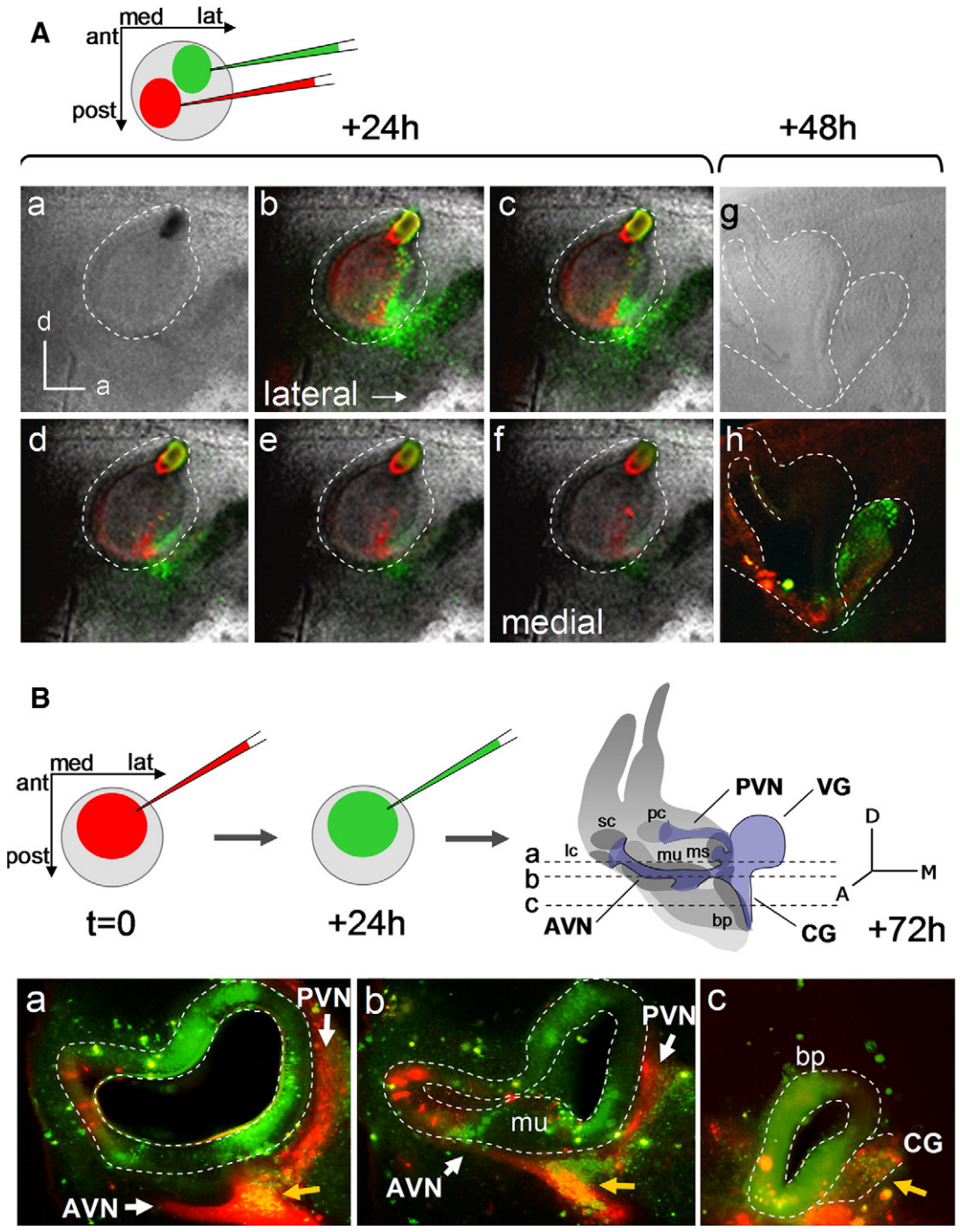

Fig. 3. Injections of DiI and DiO reveal the timing of neurogenesis. (A) DiI (medial) and DiO (lateral) were injected simultaneously in distinct domains of HH12 (E2) otic placodes. Embryos were allowed to grow for 24 h (a–f) and 48 h (g, h), and examined using confocal microscopy. Panels Aa–f are photographs of serial sections at 10 μm intervals from lateral to medial, showing that DiO labelled cells have migrated out of the otic vesicle, while DiI-labelled cells remain in the otic epithelium. Panels Ag–h, confocal projections of a similar experiment 48 h after labelling; DiO positive cells are found more distally than DiI-labelled cells. (B) The otic neurogenic region was sequentially labelled with DiI and DiO (top): DiI (red) was injected at stage HH13 (E2), the same embryo was injected with DiO (green) at HH18 (E3). Embryos were allowed to develop to HH23 (E4–5) and sectioned. The levels of the sections shown in panels a–c are indicated in the diagram. The yellow arrows indicate overlapping regions of DiI and DiO. Note that the dorsal domain of the vestibular ganglion is only labelled by DiI but not by DiO, while its ventral part and the cochlear ganglion are labelled by both, indicating that dorsal CVG neurons are produced before ventral neurons. mu: macula utriculi, bp: basilar papilla, AVN: anterior vestibular nerve, PVN: posterior vestibular nerve. VG: vestibular ganglion, CG: cochlear ganglion.

Origin of the sensory epithelia

Next, we investigated whether sensory precursors of the inner ear are also spatially segregated. The position of the precursors for the different sensory organs in the otic placode was determined by matching the original injections to labelled cells in the sensory epithelia (Fig. 4). The domains were identified morphologically as anterior, lateral and posterior cristae (yellow, orange, and pink, respectively in Fig. 4), maculae (purple) and the basilar papilla (green). As mentioned above, the structure and innervation of the macula utriculi could not easily be distinguished from the macula sacculi and they were pooled together for this analysis.

Nearly 75% of all injections (141/189) between HH10 and HH12 showed labelling of one or more sensory patch and an ordered distribution of progenitors for different sensory organs within the otic placode was apparent (Fig. 4A). The fate maps (Fig. 4A) reveal that precursors for anterior and lateral cristae (AC and LC, yellow and orange; see also Figs. 1C, Ea) are located in the anterior and lateral domain of the otic placode, whereas precursors for posterior cristae (PC, pink) and for maculae (M, purple; see also Fig. 1Ed) cluster more medially. Future basilar papilla cells (Fig. 4A BP, green; see also Fig. 1Ee) are most often found in the posterior-medial part of the otic cup. Although it is possible to label any of the sensory patches at all stages examined, earlier injections more readily label anterior vestibular structures, while slightly later injections label PC and BP more often. The majority of injections (84%; 118/141) label just one or two sensory patches with most (60%; 84/141) showing staining in just one sensory epithelium (Fig. 4B, C coloured regions). Precursors for the basilar papilla seem to overlap only with those for the maculae, but never with any cristae (Fig. 4B). Thus, like neuronal precursors, progenitors for the sensory epithelia appear to be spatially segregated along the anterior-lateral/posterior-medial axis of the otic placode.

Relationship between sensory and neuronal precursors

The fate maps suggest a spatial relationship between the position that cells occupy within the proneural domain and their final location, both in different sensory organs and in the ganglion. Do neurons and the sensory cells they innervate arise from the same position in the otic placode? This indeed seems to be the case (Fig. 5). Single injections in the lateral otic placode at HH10 give rise to labelled cells in both the anterior and lateral cristae and the neurons that project to them. Likewise, labelled cells in the posterior-medial portion of the otic placode contribute to the CG and the sensory cells of the basilar papilla. To analyse this in more detail we analysed the frequency with which a single injection simultaneously labels a specific neuron and its target (Fig. 5). Overall, Chi squared (χ^2) tests of the probability of the bias towards co-labelling of a particular neuronal population and the corresponding sensory epithelium gave significant values for all groups ($p<5\times10^{-10}$, data from Fig. 5B). This is the case in at least 68% cases (with respect to the sensory epithelia), for which it is at least twice as likely as any other combination. Some combinations are rarely observed such as co-labelling of the lateral cristae and the cochlear ganglion (13%) or the basilar papilla with the anterior-lateral vestibular ganglion (22%). This analysis indicates that neuronal precursors are most likely to originate from the same domain as the sensory organs they will eventually innervate.

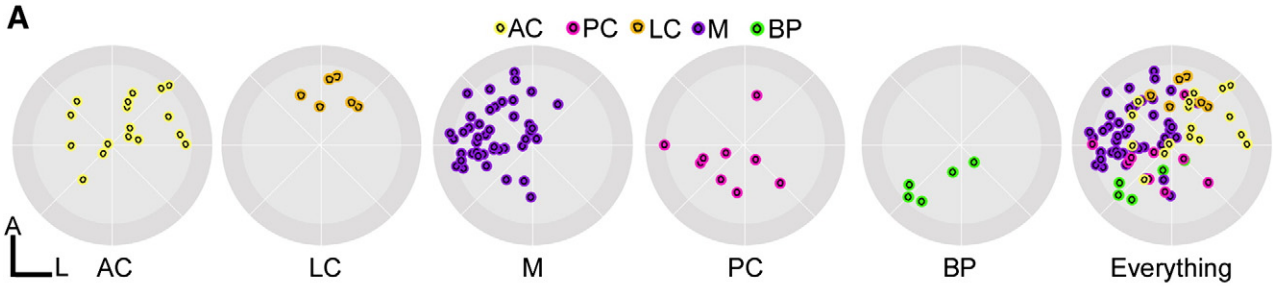

B

n		AC	LC	PC	M	BP
41	AC	17				
24	LC	4	6			
39	PC	3	0	9		
95	M	5	6	12	50	
18	BP	0	0	0	6	5

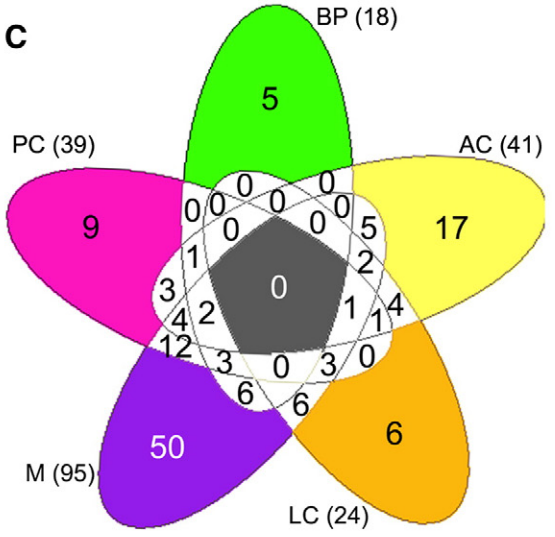

Fig. 4. The origin of the sensory organs in the otic placode. (A) Panels showing the position of sensory organ precursors in the otic placode at HH10–12 (E1.5–2). Only injections that gave rise to labelling of a single sensory patch are shown. Data are equivalent to those represented in the coloured boxes/petals in panels B and C. AC yellow, LC orange, M purple, PC pink, BP green. (B) Table showing the frequency of how often a particular sensory patch is co-labelled with another sensory patch. n: total number of labels scored. (C) Venn diagram showing the frequency of labels in all epithelial combinations.

A

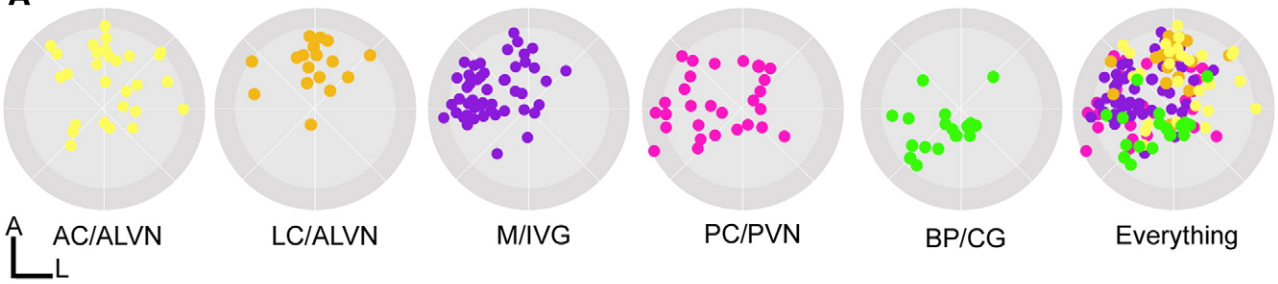

B

Nerve branch	Sensory Epithelium (n) AC (41)	LC (24)	PC (39)	M (95)	BP (18)
ALVN	28(68%)	17(71%)	17(44%)	34(36%)	4(22%)
PVN	13(32%)	6(25%)	28(72%)	42(44%)	7(39%)
IVG	8(20%)	9(38%)	17(44%)	65(68%)	7(39%)
CG	11(27%)	3(13%)	12(31%)	20(21%)	14(78%)

Fig. 5. Corresponding locations of neuronal and sensory organ precursors. (A) Maps showing those samples where a single injection labelled a particular sensory patch as well as the nerve that innervates it, regardless of whether other nerve branches or sensory epithelia were also labelled. The data shown correspond to data in the coloured boxes in panel B. AC/ALVN: yellow, LC/ALVN: orange, M/IVG: purple, PC/PVN: pink, BP/CG: green. (B) Table showing the frequency of injections labelling different combinations of nerve branch and sensory epithelium. The percentage is calculated against the total number of labels seen in a particular sensory patch. n: total times a label was scored in a particular sensory patch regardless of whether other patches were also labelled.

NeuroD and NeuroM are transiently expressed in vestibular and cochlear neuroblasts

To correlate the fate maps with the expression of neuronal markers at different stages of maturation, we studied the expression of *NeuroD* and *NeuroM* in the otic primordium, from neuroblast generation (HH12; E2) to the segregation of the cochlear and vestibular ganglia (HH30–31; E7). *NeuroD* and *NeuroM* are first detected in very few cells in the most anterior and lateral domain of the early otic cup at HH12 and invade the anterior-medial region by HH13 (Figs. 6A–D). *NeuroM*$^+$ cells are initially more abundant than *NeuroD*$^+$ neuroblasts (Figs. 6A, B). Serial sagittal sections (Figs. 6Ea–d for *NeuroD* and Fa–d for *NeuroM*), illustrate that *NeuroD*$^+$ neuroblasts are confined to the otic epithelium, while *NeuroM* is also expressed in neuroblasts delaminating from the ventral otic cup (arrow in Fig. 6Fb). During late otic cup and vesicle stages (HH15–21), both *NeuroM* and *NeuroD* are detected in the otic epithelium and in neuroblasts that migrate to form the CVG (Figs. 6G–K for *NeuroD* and L–P for *NeuroM*). Over time, the number of cells expressing each gene increases as expected from a period of intense neuronal production (D'Amico-Martel, 1982). However, their precise expression domains differ slightly in that *NeuroD* remains expressed in neuroblasts within the epithelium and close to the otic cup (Figs. 6J and K), while *NeuroM*$^+$ neuroblasts are less abundant in the epithelium and concentrate at the distal edge of the developing ganglion (Fig. 6P). Thus, the expression patterns of *NeuroM and NeuroD* parallel the sequence of neuroblasts delamination and suggest that neurogenesis in the otic placode progresses with time from anterior-lateral to medial. Moreover, the expression of both genes is similar, with *NeuroM* slightly preceding *NeuroD* expression.

By HH24 (E4), both *NeuroM* and *NeuroD* are still expressed in the developing CVG as well as in delaminating neuroblasts (Figs. 6Qa–c and Ra–c). However, the most dorsal and lateral aspect of the CVG, which corresponds to the vestibular ganglion, shows little or no expression of either transcript (Figs. 6Qa and Ra), while both genes are intensely expressed in the ventral and medial domain of the CVG, corresponding to the macular and cochlear components (Figs. 6Qb–c and Rb–c). Delamination from the otic epithelium is still ongoing throughout these stages in the region that corresponds to the utricular macula (arrowheads in Figs. 6Qa and Ua; see also Cole et al., 2000; Matei et al., 2005). From HH27 (E5) onwards, the CVG is split into two distinct components: the ventral portion close to the developing basilar papilla, and another more dorsal neuronal condensation close to the utricule–saccule ventricle, the vestibular ganglion (see diagram in Fig. 1). Alternate transverse sections show that *NeuroM* and *NeuroD* are absent from the vestibular and the cochlear ganglion from HH27 onwards (Figs. 6Sa–c Ta–c for E5, Ua–c for E6), except for neuroblasts delaminating close to the macular epithelium (inset in Fig. 6Sc, arrowhead in Fig. 6Ua). Thus, *NeuroD* and *NeuroM* are expressed transiently in both neuronal subtypes of the ear.

NeuroD and NeuroM precede neuronal differentiation

The above results suggest that *NeuroD* and *NeuroM* do not label different neuronal subtypes, but rather identify nascent neuroblasts. Their temporal expression coincides with neuroblast production and ceases with the last cell division, as neuronal differentiation begins (D'Amico-Martel, 1982). This is confirmed by comparing their expression with neuronal differentiation markers. Islet1 and Tuj1 are expressed in a complementary pattern to *NeuroD* and *NeuroM* in the CVG as illustrated by combined *in situ* hybridisation and immunolabelling (Figs. 7A–C). The expression of Islet1 is always dorsal and distal to *NeuroM* and corresponds to the first-born neurons, which exit the cell cycle between HH17 (E2.5) and HH18 (E3) (D'Amico-Martel, 1982). Likewise, the expression of both proneural genes is complementary to Tuj1 (Figs. 7D–I), although a small overlap is observed (Figs. 7F, I).

We also compared the expression of proneural genes with that of the neurotrophin receptor *TrkC (Nrtk3)*, which in chick is prominently expressed in early differentiated otic neurons (Cochran et al., 1999). *TrkC* mRNA is already detected at the otic cup stage (HH14; Fig. 7J), corresponding to the generation of the earliest vestibular neurons (D'Amico-Martel, 1982). Unlike *NeuroM* and *NeuroD*, *TrkC* is not expressed in the otic cup or newly delaminating neuroblasts (Fig. 7J), indicating that differentiation does not start until neuroblasts leave the otic epithelium. During otic vesicle stages, *TrkC* is expressed in the

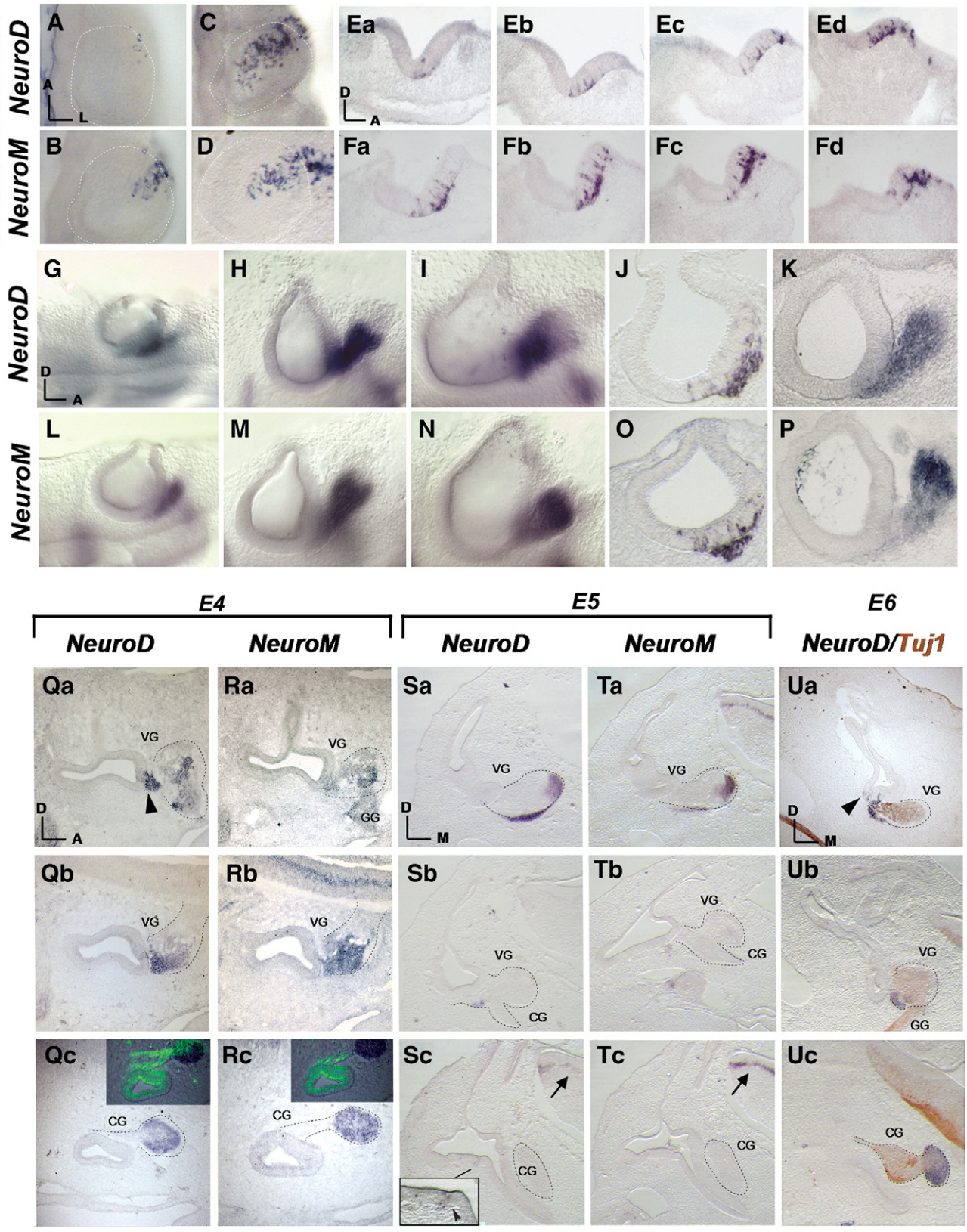

Fig. 6. *NeuroM* and *NeuroD* expression throughout otic neurogenesis. *In situ* hybridisation showing *NeuroD* and *NeuroM* during the development of the CVG. (A, B) Dorsal views of otic cups at HH12. (C, D) Dorsal views of otic cups at HH13. (Ea–Ed and Fa–Fd). Sagittal sections of HH12^{+} otic cups from medial (Ea, Fa) to lateral (Ed, Fd). Arrow in panel Fb points to neuroblasts in the CVG. (G–I) Lateral views of developing inner ears from HH15 (G), HH18 (H) and HH20 (I) embryos stained for *NeuroD*. (L–N) Lateral views of developing inner ears from HH16 (L), HH18 (M) and HH21 (N) embryos stained for *NeuroM*. (J, K) Sagittal sections showing expression of *NeuroD* at HH17 (J) and HH18 (K). (O, P) Sagittal sections showing expression of *NeuroM* at HH17 (O) and HH18 (P). (Qa–Qc (*NeuroD*) and Ra–Rc (*NeuroM*)) Sagittal sections of HH24 (E4) stage otic vesicles shown from lateral (Qa, Ra) to medial (Qc, Rc). Inset in panels Qc and Rc show double staining of *NeuroD* or *NeuroM* transcripts and Tuj1 (green) in the CG innervating the basilar papilla. (Sa–Sc and Ta–Tc) Transverse sections of HH27 (E5) otocysts shown from posterior (Sa, Ta) to anterior (Sc, Tc). Inset in panel Sc shows expression of *NeuroD* in the neuroblasts of the otic epithelium; arrows in panels Sc and Tc indicate *NeuroM* and *NeuroD* expression in the hindbrain. (Ua–Uc) Double staining of *NeuroD* and Tuj1 in HH31 (E6) otocysts shown in sagittal sections. Arrowhead points to *NeuroD* expressing cells delaminating from the utricular macula.

CVG and overlaps with the distal-most front of *NeuroM* expression (compare *TrkC* in Figs. 7K and L, with *NeuroD* and *NeuroM* in Figs. 6I and N). Alternate sections (Figs. 7M–O) show that like Islet1 and Tuj1, *TrkC* expression is complementary to *NeuroM* and *NeuroD*, although a transition zone expressing both proneural and neurotrophin receptor mRNAs is apparent (Figs. 7M–O). In summary, gene expression patterns reflect a temporal pattern of neuron generation in which young neuroblasts first populate the superior vestibular ganglion around HH17–18 (E3–3.5) and differentiate early. Subsequently, from HH23 (E4) onwards, neurons that innervate the maculae and basilar papilla are generated. None of the genes examined appears to be restricted to vestibular or cochlear neurons.

Discussion

The vertebrate inner ear has a complex architecture and generates a variety of different cell types including sensory cells and the neurons that innervate them. Its development from a simple epithelium, the otic placode, therefore requires precise coordination of cell fate specification and morphogenesis. The first cells specified are otic neurons, which derive from the anterior-medial region of otic placode (Alsina et al., 2004), from where they delaminate to form the CVG (D'Amico-Martel and Noden, 1983; Adam et al., 1998). The CVG develops further into two separate parts containing the primary afferent neurons of the auditory and vestibular components of the

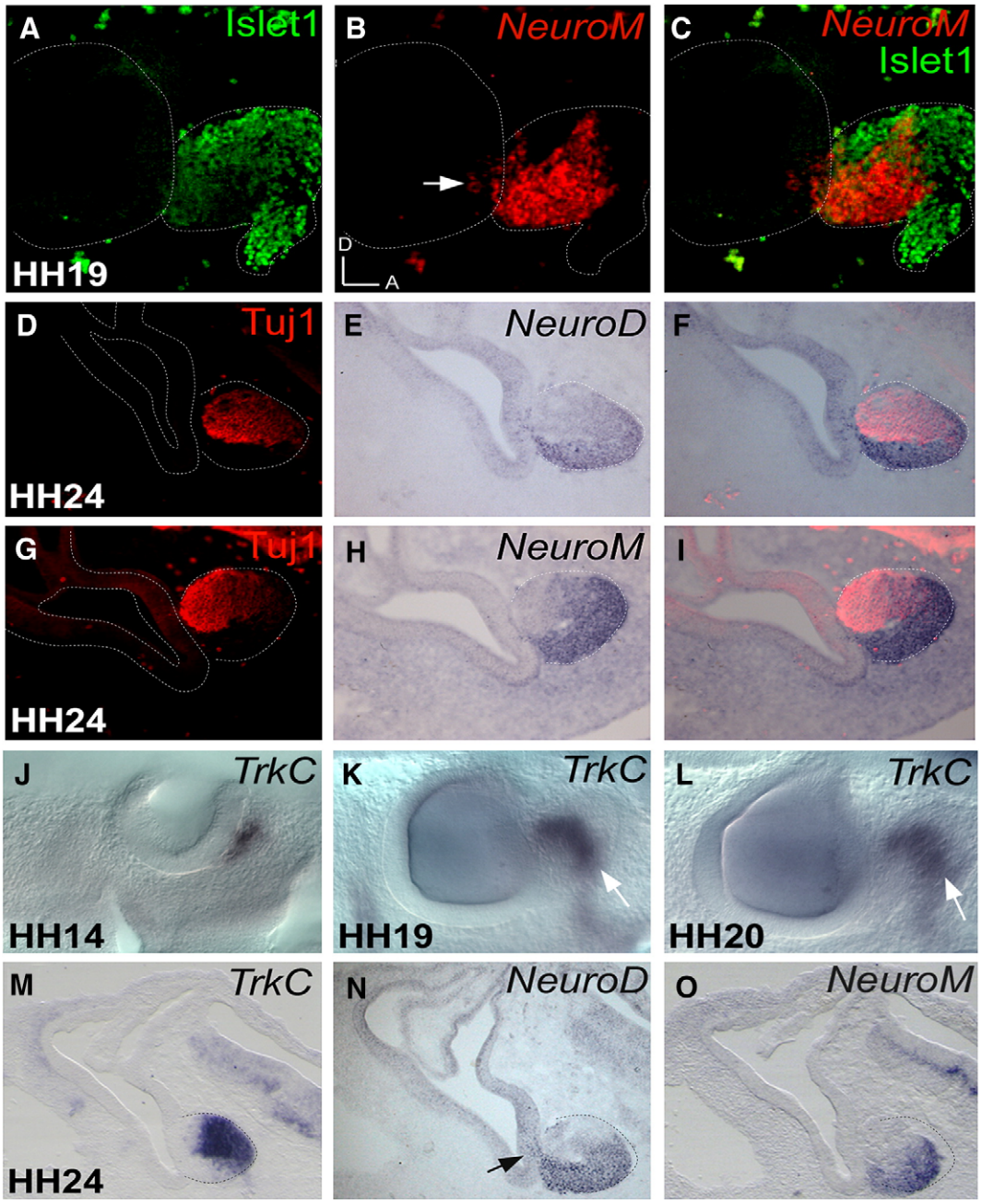

Fig. 7. *NeuroM* and *NeuroD* expression during otic neurogenesis and differentiation. Comparison of *NeuroD* and *NeuroM* expression with neuronal differentiation markers. (A–C) Sagittal sections of HH19 otic vesicles double-labelled with *NeuroM* (fluorescence RNA *in situ* hybridisation, red) and Islet1 (immunohistochemistry, green). Arrow in panel B points to delaminating neuroblasts. (D–I) Alternate sagittal sections of HH24 otocysts stained for *NeuroD* and TUJ1 (D–F) and for *NeuroM* and TUJ1 (G–I). Note that proneural gene expression is complementary to neurofilament staining. (J–L) Lateral views of *TrkC* expression during otic development. At HH14 (J) a small population of neuroblasts already expresses *TrkC*. This population remains distal to the otic epithelium at HH19 (K, arrow) and HH20 (L, arrow). (M–O) Sagittal sections of HH24 stage otocysts showing complementary expression of *TrkC* (M), *NeuroD* (N) and *NeuroM* (M). OV: otic vesicle. CVG: cochlear–vestibular ganglion.

inner ear. These neurons project peripherally towards corresponding sensory organs and centrally towards the brainstem (Rubel and Fritzsch, 2002). Our results show four key components of otic sensorineuronal development. First, although partially overlapping, precursors for different sense organs and innervating neurons are segregated along the anterior–posterior axis of the otic placode. Second, neuronal progenitors and the sensory cells they later innervate are generated in close proximity. Third, delamination of neuroblasts, which innervate different sensory patches, occurs in a temporal (as well as spatial) manner and, finally, we show that the dynamic expression of *NeuroD* and *NeuroM* reflects the timing of neuroblast production but not different neuronal subtypes. We propose that the development of different sensory organs and their corresponding innervation depends on spatial and temporal cues that are coordinated at the otic placode stage, such that a wave of differentiation proceeds from anterior-lateral towards posterior-medial to result in an ordered generation of vestibular and cochlear sensory organs and neurons (Fig. 8).

Progenitors for vestibular and cochlear neurons are spatially segregated in the otic placode

Our results show a spatial segregation of neuronal precursors in the otic placode that is maintained throughout neuroblast delamination, expansion and migration to their final positions. Vestibular progenitors, innervating the anterior and lateral cristae, are located in the anterior-lateral proneural region, those innervating maculae and posterior cristae are found in its anterior-medial part while cochlear precursors are concentrated posterior-medially. Even when neighbouring cell populations are labelled in the otic placode, only limited intermingling is observed and the respective labels are found in adjacent groups of neurons and fibres at later stages. That neuronal precursors segregate early is further supported by the finding that single cells rarely contribute progeny to both the cochlear and the vestibular ganglia, but mostly to just one of these (Satoh and Fekete, 2005). These findings suggest that positional information imparts neuronal identity in the chick. In contrast, in *Xenopus* extensive cell movements in the otic placode and vesicle have been described and a single region can contribute to multiple sensory organs, including cells that apparently disperse from anterior to posterior poles and vice-versa (Kil and Collazo, 2001). Whether these observations reflect species or experimental differences remains to be determined.

Otic neurons already begin to extend processes towards the developing sensory epithelia before they have reached their definitive position within the ganglion and before they form a central process (Rubel and Fritzsch, 2002; Fekete and Campero, 2007). Recent studies in mouse show that discrete populations of *Neurog1*$^{+}$ cochlear progenitors establish stereotyped connections to their targets depending on their birth date, but independent of their interactions with hair cells (Koundakjian et al., 2007). Therefore, otic axon guidance seems to depend on intrinsic cues, indicating that the bias to innervate specific targets of the ear occurs very early during neurogenesis. The spatial segregation of precursors for different neuronal subtypes, as indicated by our fate maps, also suggests such

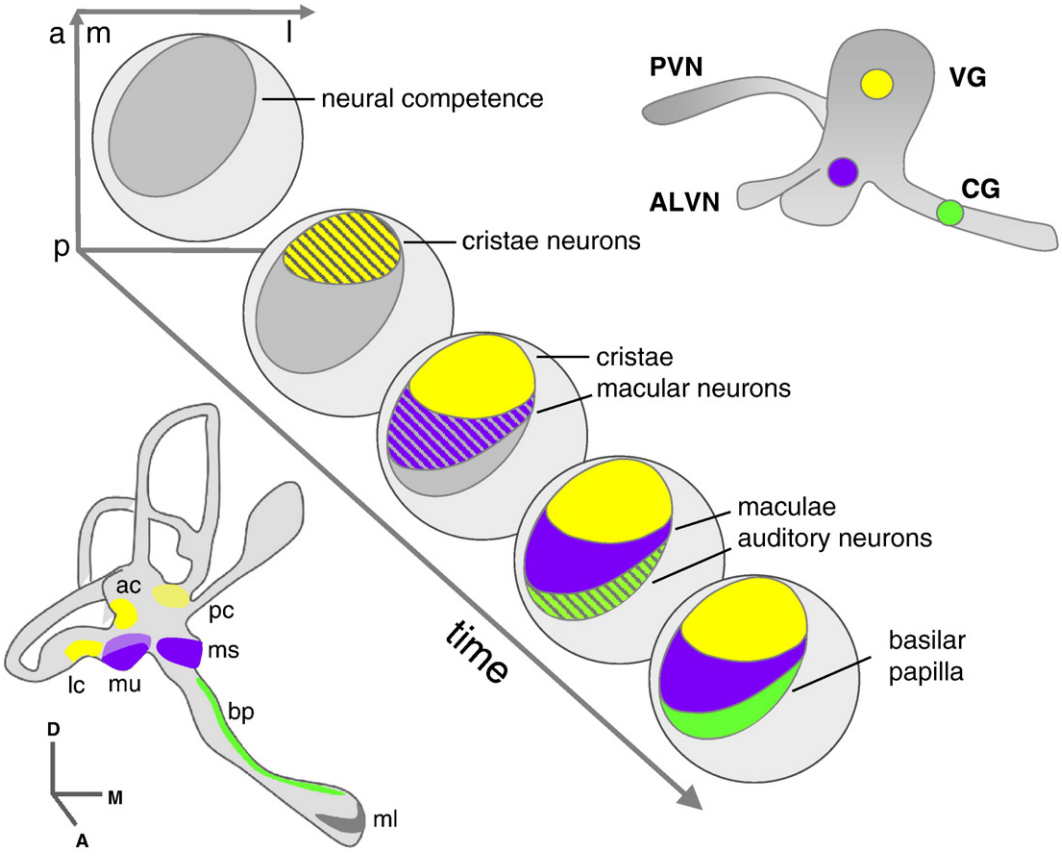

Fig. 8. Model for coordination of spatial and temporal cues during fate determination. The diagram illustrates the development of the otic placode throughout time from upper-left to lower-right. The mature inner ear with colour-coded sensory patches (cristae = yellow, maculae = purple, and basilar papilla = green) is shown in the lower left. The CVG is represented in the upper right with the neurons colour-coded according to the sensory organs they innervate. The neural competent domain in grey gives rise to the different neural precursors, neurons and sensory organs. Vestibular neurons targeting cristae are specified first in the most anterior and lateral domain of the otic placode (yellow with blue stripes), followed by macular neurons more medially (purple with blue stripes) and, finally by cochlear neurons from the most posterior and medial domains of the otic placode (green with blue stripes). As neurons are specified, the same domains differentiate later into the corresponding sensory patch. In this cartoon, all cristae have been pooled to simplify the diagram, however it is likely that anterior and lateral cristae are segregated from posterior crista.

early specification. However, the fact that precursors of sense organs and their innervating neurons can be distinguished at placode stages, does not imply that they are committed to their fate. Commitment of neural competent otic progenitors to their definitive fates seems to follow a stereotyped time profile (see below). Nevertheless, together, these observations suggest that positional information is at least one essential mechanism by which neuronal subtype specification takes place in the inner ear.

Sensory organs and neurons derive from a common domain

The question of whether otic sensory cells and the neurons that innervate them originate next to each other or from separate domains has been extensively debated in the literature (for review see: Rubel and Fritzsch, 2002; Fekete and Campero, 2007). Our results show that sensory organs and their corresponding neurons originate from the same location in the otic placode and in a significant proportion both are labelled with the same injection. Although we cannot draw conclusions about lineage relationships, these results are in agreement with the observation that chick vestibular neurons and macular sensory epithelia are clonally related (Satoh and Fekete, 2005). Likewise, in mouse macular neurons and hair cells derive from a common *Neurog1*$^+$ domain (Raft et al., 2007). *Neurog1* expression contracts parallel to the production of neurons, while *Atoh1* expression expands concomitant with the birth of hair cells, suggesting that the same region first produces neurons, and subsequently generates sensory cells. Our results suggest that a similar relationship may exist for other neuronal and sensory precursors in the ear. In contrast, results in mice show that the cristae and cochlear sensory epithelium appear to form in a *Neurog1*-independent manner (Koundakjian et al., 2007; Raft et al., 2007) and may therefore lack of neurogenic potential. This discrepancy may indicate species-specific differences between chick and mouse, but it is also possible that cristae are generated earlier than explored in the genetic labelling experiments (Koundakjian et al., 2007; Raft et al., 2007) or, perhaps less likely, that a yet unidentified gene with proneural function may substitute *Neurog1* in other sensory organs. An alternative explanation for the discrepancy between mouse and chick is that the *Neurog1*+ macular domain contains precursors for the neurons innervating cristae and basilar papilla, which in turn partially overlap with progenitors for the sensory cells themselves. This possibility implies that neurogenic and sensory maps are superimposed in the otic placode. Neuronal and non-neuronal precursors may be intermingled at the edge of the prospective maculae, but do not necessarily share a common lineage.

How do otic neurons connect to the same sites of the epithelium from where they originate to innervate corresponding hair cells? Our experiments do not address this question directly, but do show that there is little cell mixing between the progeny of neighbouring cells. In mouse, type I and type II neurons appear to follow intrinsic, stereotyped patterns to innervate their targets as soon as they are specified (Koundakjian et al., 2007). The molecular mechanisms that maintain such fibre organisation are unknown. As discussed by Fekete and Campero (2007) two possible mechanisms could guide otic fibres to their sensory targets: a “reverse pathfinding mechanism” by which neuronal projections return to the innervation sites following their original migratory pathway, or specific long-range chemoattractants released by sensory organs. One possible mechanism for reverse pathfinding is that although neurons delaminate from the otic epithelium, they may leave a fine trailing process behind along which they project back (see Ruben and Fritzsch, 2002).

The temporal sequence of neurogenesis and sensory cell formation in the otic epithelium

Classical studies demonstrated that vestibular neurons withdraw from the cell cycle between E2 and E3, while cochlear neurons undergo a final mitosis between E4 and E5 (D'Amico-Martel, 1982). Our results show that a temporal sequence of neurogenesis is superimposed onto the regional segregation of precursors so that vestibular neurons are generated prior to cochlear neurons. Indeed, a recent study in mouse also shows that the early *Neurog1*$^+$ population contributes to vestibular neurons, while the late *Neurog1*$^+$ domain generates cochlear neurons (Koundakjian et al., 2007). This suggests that neuronal subtype determination may depend on the coordination of spatial and temporal cues.

The sequential production of neuroblasts that innervate different targets is paralleled by the sequential differentiation of sensory organs (Ruben, 1967; D'Amico-Martel, 1982; Whitehead and Morest, 1985). In mouse and chick, the analysis of molecular markers suggests that cristae are generated first, followed by maculae and finally by cochlear sensory cells (Wu and Oh, 1996; Morsli et al., 1998; Chen et al., 2002; Mantela et al., 2005). Thus, synchronisation of sensory cells and their innervating neurons at early stages, when they are closely associated in space, may be a key step to match neurons with their targets.

The temporal pattern of neurogenesis is mirrored by sequential expression of proneural genes in different parts of the otic placode. *NeuroM* and *NeuroD* expression is first observed in the anterior-lateral aspect of the otic placode, which generates precursors of the VG, and then invades medial and posterior domains of the otic cup, where cochlear neurons arise. Subsequently, both genes are found in delaminating neuroblasts and finally disappear as neurons differentiate. The expression of *NeuroD* and *NeuroM* is consistent with their known role as proneural genes (Kim et al., 2001; Bertrand et al., 2002). Interestingly, their expression patterns are overlapping but not identical with *NeuroM* being expressed prior to *NeuroD.* Likewise, in the spinal cord, *NeuroM* expression is transient and precedes that of *NeuroD* (Roztocil et al., 1997). During otic neuroblast delamination *NeuroM* is found in distal neuroblasts and lost from the otic epithelium, while *NeuroD* remains in the epithelium and in neuroblasts located close to the otocyst. Does this differential expression reflect the generation of different neuronal subtypes or a temporal sequence of neuronal differentiation? Our results indicate that auditory and vestibular ganglia transiently express both genes suggesting that their differential expression does not code for different neuronal subtypes. We therefore propose that in accordance with the fate maps, differential expression of *NeuroD* and *NeuroM* reflects intrinsic timing of neuronal differentiation in the inner ear and does not relate to the identity of otic neurons.

A model for coordination of space and time during ear development

Here, we provide evidence that otic neurons and their sensory targets arise from a common proneural domain, in which different precursors are spatially segregated. The dorsal/ventral axis of the ear is spatially represented in the placode with dorsal (cristae) being located in the anterior and lateral domain, ventral (cochlear) in the posterior and medial region, and with the maculae in an intermediate position. At the same time, generation of both sensory organs and neurons follows a stereotyped temporal sequence, so that neurons precede sensory organ formation, and the vestibular system precedes development of cochlear structures. To integrate these findings into a common framework, we propose a model (Fig. 8), in which a wave of differentiation sweeps across the otic cup from anterior-lateral to posterior-medial. Vestibular neurons targeting cristae are specified first in the most anterior and lateral domain of the otic placode (yellow–blue stripes), followed by macular neurons more medially (purple–blue stripes) and finally by cochlear neurons from the most posterior and medial domain (green–blue stripes). As neurons are specified, the same domains differentiate into corresponding sensory patches (loss of blue stripes) to match the time of neuron and sensory differentiation. Although spatial relationships are likely to be more complex and dynamic during the transition

from the placode to the otocyst the model predicts that time and position impart an intrinsic code to delaminating neurons that later allows target recognition.

Acknowledgments

We are indebted to Ewa Kolano for technical assistance; thanks to C.D. Stern, C. Pujades and Y. León for critical reading of the manuscript. This work was funded by grants from the Guy's and St Thomas' Charitable Foundation and the BBSRC to AS, BMC2002-00355 CICYT to BA, BFU2005-0084-CICYT and CSIC to IVN, and XT-G03/203 ISCIII MSC to IVN and FG. IG was supported by a predoctoral fellowship from the Eusko Jaularitza.

References

Abelló, G., Khatri, S., Giraldez, F., Alsina, B., 2007. Early regionalization of the otic placode and its regulation by the notch signaling pathway. Mech. Dev. 124, 631–645.

Adam, J., Myat, A., Le Roux, I., Eddison, M., Henrique, D., Ish-Horowicz, D., Lewis, J., 1998. Cell fate choices and the expression of notch, delta and serrate homologues in the chick inner ear: parallels with *Drosophila* sense-organ development. Development 125, 4645–4654.

Alsina, B., Giraldez, F., Varela-Nieto, I., 2003. Growth factors and early development of otic neurons: interactions between intrinsic and extrinsic signals. Curr. Top. Dev. Biol. 57, 177–206.

Alsina, B., Abello, G., Ulloa, E., Henrique, D., Pujades, C., Giraldez, F., 2004. FGF Signaling is required for determination of otic neuroblasts in the chick embryo. Dev. Biol. 267, 119–134.

Altman, J., Bayer, S.A., 1982. Development of the cranial nerve ganglia and related nuclei in the rat. Adv. Anat. Embryol. Cell Biol. 74, 1–90.

Bertrand, N., Castro, D.S., Guillemot, F., 2002. Proneural genes and the specification of neural cell types. Nat. Rev. Neurosci. 3, 517–530.

Campuzano, S., Modolell, J., 1992. Patterning of the *Drosophila* nervous system: the achaete–scute gene complex. Trends Genet. 8, 202–208.

Carney, P.R., Silver, J., 1983. Studies on cell migration and axon guidance in the developing distal auditory system of the mouse. J. Comp. Neurol. 215, 359–369.

Chen, P., Johnson, J.E., Zoghbi, H.Y., Segil, N., 2002. The role of Math1 in inner ear development: uncoupling the establishment of the sensory primordium from hair cell fate determination. Development 129, 2495–2505.

Cochran, S.L., Stone, J.S., Bermingham-McDonogh, O., Akers, S.R., Lefcort, F., Rubel, E.W., 1999. Ontogenetic expression of Trk neurotrophin receptors in the chick auditory system. J. Comp. Neurol. 413, 271–288.

Cole, L.K., Le Roux, I., Nunes, F., Laufer, E., Lewis, J., Wu, D.K., 2000. Sensory organ generation in the chicken inner ear: contributions of bone morphogenetic protein 4, serrate1, and lunatic fringe. J Comp. Neurol. 424, 509–520.

D'Amico-Martel, A., 1982. Temporal patterns of neurogenesis in avian cranial sensory and autonomic ganglia. Am. J. Anat. 163, 351–372.

D'Amico-Martel, A., Noden, D.M., 1983. Contributions of placodal and neural crest cells to avian cranial peripheral ganglia. Am. J. Anat. 166, 445–468.

Fekete, D.M., Campero, A.M., 2007. Axon guidance in the inner ear. Int. J. Dev. Biol. 51, 549–556.

Germroth, P.G., Gourdie, R.G., Thompson, R.P., 1995. Confocal microscopy from acrylamide gel embedded embryos. Microscopy Res. and Technique 30, 513–520.

Henrique, D., Adam, J., Myat, A., Chitnis, A., Lewis, J., Ish-Horowicz, D., 1995. Expression of a delta homologue in prospective neurons in the chick. Nature 375, 787–790.

Kil, S.H., Collazo, A., 2001. Origins of inner ear sensory organs revealed by fate map and time-lapse analyses. Dev. Biol. 233, 365–379.

Kim, W.Y., Fritzsch, B., Serls, A., Bakel, L.A., Huang, E.J., Reichardt, L.F., Barth, D.S., Lee, J.E., 2001. NeuroD-Null mice are deaf due to a severe loss of the inner ear sensory neurons during development. Development 128, 417–426.

Koundakjian, E.J., Appler, J.L., Goodrich, L.V., 2007. auditory neurons make stereotyped wiring decisions before maturation of their targets. J. Neurosci. 27, 14078–14088.

Lee, S.K., Pfaff, S.L., 2003. Synchronization of neurogenesis and motor neuron specification by direct coupling of bHLH and homeodomain transcription factors. Neuron 38, 731–745.

Liu, M., Pereira, F.A., Price, S.D., Chu, M.J., Shope, C., Himes, D., Eatock, R.A., Brownell, W.E., Lysakowski, A., Tsai, M.J., 2000. Essential role of BETA2/NeuroD1 in development of the vestibular and auditory systems. Genes Dev. 14, 2839–2854.

Ma, Q., Anderson, D.J., Fritzsch, B., 2000. Neurogenin 1 null mutant ears develop fewer, morphologically normal hair cells in smaller sensory epithelia devoid of innervation. J. Assoc. Res. Otolaryngol. 1, 129–143.

Mantela, J., Jiang, Z., Ylikoski, J., Fritzsch, B., Zacksenhaus, E., Pirvola, U., 2005. The retinoblastoma gene pathway regulates the postmitotic state of hair cells of the mouse inner ear. Development 132, 2377–2388.

Matei, V., Pauley, S., Kaing, S., Rowitch, D., Beisel, K.W., Morris, K., Feng, F., Jones, K., Lee, J., Fritzsch, B., 2005. smaller inner ear sensory epithelia in Neurog 1 null mice are related to earlier hair cell cycle exit. Dev. Dyn. 234, 633–650.

Morsli, H., Choo, D., Ryan, A., Johnson, R., Wu, D.K., 1998. development of the mouse inner ear and origin of its sensory organs. J. Neurosci. 18, 3327–3335.

Noden, D.M., van de Water, T.R., 1986. The developing ear: tissue origins and interactions. In: Ruben, R.J., van de Water, T.R., Rubel, E.W. (Eds.), The Biology of Change in Otolaryngology. Elsevier, Amsterdam, pp. 15–46.

Parras, C.M., Schuurmans, C., Scardigli, R., Kim, J., Anderson, D.J., Guillemot, F., 2002. divergent functions of the proneural genes Mash1 and Ngn2 in the specification of neuronal subtype identity. Genes Dev. 16, 324–338.

Raft, S., Koundakjian, E.J., Quinones, H., Jayasena, C.S., Goodrich, L.V., Johnson, J.E., Segil, N., Groves, A.K., 2007. Cross-regulation of Ngn1 and Math1 coordinates the production of neurons and sensory hair cells during inner ear development. Development 134, 4405–4415.

Roztocil, T., Matter-Sadzinski, L., Alliod, C., Ballivet, M., Matter, J.M., 1997. NeuroM, a neural helix–loop–helix transcription factor, defines a new transition stage in neurogenesis. Development 124, 3263–3272.

Rubel, E.W., Fritzsch, B., 2002. Auditory system development: primary auditory neurons and their targets. Annu. Rev. Neurosci. 25, 51–101.

Ruben, R.J., 1967. Development of the inner ear of the mouse: a radioautographic study of terminal mitoses. Acta Otolaryngol. Suppl 220, 1–44.

Sanchez-Calderon, H., Milo, M., Leon, Y., Varela-Nieto, I., 2007. A network of growth and transcription factors controls neuronal differentation and survival in the developing ear. Int. J. Dev. Biol. 51, 557–570.

Satoh, T., Fekete, D.M., 2005. Clonal analysis of the relationships between mechanosensory cells and the neurons that innervate them in the chicken ear. Development 132, 1687–1697.

Stern, C.D., 1998. Detection of multiple gene products simultaneously by in situ hybridization and immunohistochemistry in whole mounts of avian embryos. Curr. Top. Dev. Biol. 36, 223–243.

Whitehead, M.C., Morest, D.K., 1985. The development of innervation patterns in the avian cochlea. Neuroscience 14, 255–276.

Wu, D.K., Oh, S.H., 1996. sensory organ generation in the chick inner ear. J. Neurosci. 16, 6454–6462.